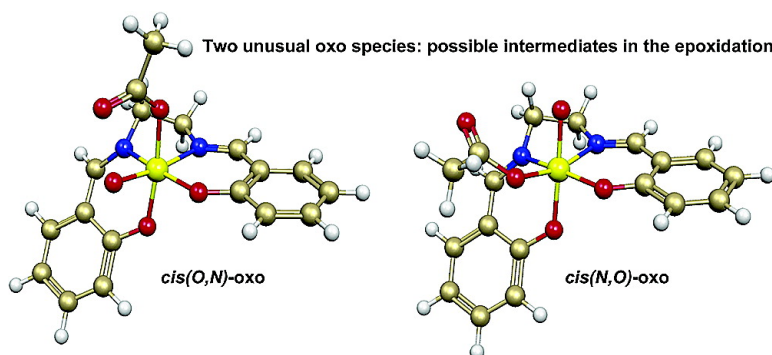## Article

Insights into the Structure and Reactivity of Acylperoxo Complexes in the Kochi–Jacobsen–Katsuki Catalytic System. A Density Functional Study

Ilja V. Khavrutskii, Djamaladdin G. Musaev, and Keiji Morokuma

Two unusual oxo species: possible intermediates in the epoxidation

cis(O,N)-oxo   *cis(N,O)*-oxo

More About This Article

Additional resources and features associated with this article are available within the HTML version:

- Supporting Information
- Links to the 5 articles that cite this article, as of the time of this article download
- Access to high resolution figures
- Links to articles and content related to this article
- Copyright permission to reproduce figures and/or text from this article

View the Full Text HTML

Insights into the Structure and Reactivity of Acylperoxo Complexes in the Kochi−Jacobsen−Katsuki Catalytic System. A Density Functional Study

Ilja V. Khavrutskii, Djamaladdin G. Musaev,* and Keiji Morokuma*

Contribution from the Cherry L. Emerson Center for Scientific Computation and Department of Chemistry, Emory University, Atlanta, Georgia, 30322

Received January 27, 2003; E-mail: dmusaev@emory.edu; morokuma@emory.edu

Abstract: Structural properties of the acylperoxo complexes [(Salen)Mn^{III}RCO$_3$] (**2**) and [(Salen)Mn^{IV}RCO$_3$] (**3**), the critical intermediates in the Kochi−Jacobsen−Katsuki reaction utilizing organic peracids or O$_2$/aldehydes as oxygen source, have been studied with the density functional theory. Four distinct isomers, ***cis(O,N)***, ***cis(N,O)***, ***cis(N,N)***, and ***trans***, of these complexes have been located. The isomer **2-*cis(O,N)*** in its quintet ground state, and nearly degenerate isomers **3-*cis(O,N)*** and **3-*cis(N,O)*** in their quartet ground states are found to be the lowest in energy among the other isomers. The O−O bond cleavage in the ***cis(O,N)***, ***cis(N,O)***, and ***trans*** isomers of **2** and **3** has been elucidated. In complex **3**, the O−O bond is inert. On the contrary, in complex **2**, the O−O bond cleaves via two distinct pathways. The first pathway occurs exclusively on the quintet potential energy surface (PES) and corresponds to heterolytic O−O bond scission coupled with insertion of an oxygen atom into an Mn−N(Salen) bond to form **2-N-oxo** species; this pathway has the lowest barrier of 14.9 kcal/mol and is 15.6 kcal/mol exothermic. The second pathway is tentatively a spin crossover pathway. In particular, for **2-*cis(O,N)*** and **2-*cis(N,O)*** the second pathway proceeds through a crucial minimum on the seam of crossing (MSX) between the quintet and triplet PESs followed by heterolytic O−O cleavage on the triplet PES, and produces unusual triplet **2-*cis(O,N)*-** and **2-*cis(N,O)*-oxo** ([(Salen)Mn^V(O)RCO$_2$]) species; this pathway requires 12.8 kcal/mol and is 1.4 kcal/mol endothermic. In contrast, for the **2-*trans*** isomer, spin crossing is less crucial and the O−O cleavage proceeds homolytically to generate **2-*trans*-oxo** [(Salen)Mn^{IV}(O)] species with RCO$_2$ radical; this pathway, however, cannot compete with that in **2-*cis*** because it needs 21.9 kcal/mol for activation and is 15.3 kcal/mol endothermic. In summary, the O−O cleavage occurs predominantly in the **2-*cis*** complexes, and may proceed either through pure high spin or spin crossover heterolytic pathway to produce **2-*cis*-oxo** and **2-N-oxo** species.

I. Introduction

Kochi−Jacobsen−Katsuki (KJK) enantioselective oxygenation of unfunctionalyzed olefins utilizing manganese-salen catalysts (salen = *N,N*-ethylene-bis-salycildeneamine) has proven to be the best route to such valuable synthetic precursors as chiral epoxides.[1−3] Success of the reaction and desire to create new and more efficient catalytic systems triggered extensive investigations of the reaction mechanism. A majority of the mechanistic studies assume that active species in the epoxidation is (Salen)Mn^V(O) oxo species postulated by Kochi et al.[1,2,4−8]

Despite a tremendous success of this hypothesis in explaining most of the experimental results, some observations do not fit into this frame. In particular, it has been shown that stereoselectivity of the epoxidation depends substantially on the oxygen source.[1,2,5−7,9−11] This strongly suggests that species other than conventional (Salen)Mn^V(O) are involved in the epoxidation in such abnormal cases. This is particularly important since one of such cases involves synthetically important class of oxidants such as organic peracids,[2,6−8,11,12] and promising systems utilizing molecular oxygen, namely a mixture of O$_2$ with aliphatic aldehydes.[11] Both oxidants are known to generate acylperoxo radicals and/or anions in situ in mild conditions.[11,13] Interest-

(1) Jacobsen, E. N. In *Catalytic Asymmetric Synthesis*, 1st ed.; Ojima, I., Ed.; VCH Publishers: New York, N. Y., 1993; pp 159−202.
(2) Jacobsen, E. N.; Wu, M. H. In *Comprehensive Asymmetric Catalysis: Asymmetric Synthesis and Induction Catalysts*; Jacobsen, E. N., Pfaltz, A., Yamamoto, H., Eds.; Springer: Berlin; New York, 1999; Vol. 2, pp 649−677.
(3) Sheldon, R. A. In *Chirotechnology: Industrial Synthesis of Optically Active Compounds*; Sheldon, R. A., Ed.; Marcel Dekker, Inc: New York, 1993; pp 322−341.
(4) Srinivasan, K.; Michaud, P.; Kochi, J. K. *J. Am. Chem. Soc.* **1986**, *108*, 2309−2320.
(5) Katsuki, T. *Coord. Chem. Rev.* **1995**, *140*, 189−214.
(6) Katsuki, T. *J. Mol. Catal. A: Chem.* **1996**, *113*, 87−107.
(7) Katsuki, T. In *Catal. Asymmetric Synth.*, 2nd ed.; Ojima, I., Ed.; Wiley-VCH: New York, N.Y., 2000, pp 287−325.

(8) Katsuki, T. *Curr. Org. Chem.* **2001**, 663−678.
(9) Palucki, M.; Pospisil, P. J.; Zhang, W.; Jacobsen, E. N. *J. Am. Chem. Soc.* **1994**, *116*, 9333−9334.
(10) Palucki, M.; McCormick, G. J.; Jacobsen, E. N. *Tetrahedron Lett.* **1995**, *36*, 5457−5460.
(11) Mukaiyama, T.; Yamada, T. *Bull. Chem. Soc. Jpn.* **1995**, *68*, 17−35.
(12) Muniz-Fernandez, K.; Bolm, C. In *Transition Metals for Organic Synthesis: Building Blocks and Fine Chemicals*; Beller, M., Bolm, C., Eds.; Wiley-VCH Verlag GmbH: Weinheim, New York, 1998; Vol. 2, pp 271−279.
(13) Kholdeeva, O. A.; Grigoriev, V. A.; Maksimov, G. M.; Fedotov, M. A.; Golovin, A. V.; Zamaraev, K. I. *J. Mol. Catal. A: Chem.* **1996**, *114*, 123−130.

ingly, applying these oxidants to the KJK reaction led to inversion of the absolute configuration of the forming epoxides,[11,14−22] compared to that obtained with conventional oxidants. However, when the oxidants were augmented with N-oxides or N-alkyl imidazoles, no inversion of the absolute configuration has been observed.[9−11,14−22] Therefore, in this particular case, acylperoxo complexes, similar to those reported earlier for the Mn−porphyrin systems,[23−25] have been proposed as the reactive intermediates, which deteriorate or even reverse the enantioselectivity.

Note that Mn−porphyrin acylperoxo complexes have been shown to react with olefins directly, as well as to undergo heterolytic or homolytic O−O bond cleavage producing new reactive oxo- and/or N-oxo species.[26−33] To elucidate the role of the (Salen)Mn-derived acylperoxo complexes in the epoxidation, a number of attempts have been made to detect them and measure their reactivity/selectivity toward different substrates by means of NMR and ESR techniques.[34−38] Despite substantial progress in this area, however, the key question of whether acylperoxo complexes are directly involved in the asymmetric induction step still remains open.

Furthermore, no structural information on the acylperoxo complexes of (Salen)Mn is available experimentally, which obscures the diversity of their transformations. To the best of our knowledge, there has been only one speculative attempt to assess the geometrical and electronic structure of (Salen)Mn-derived acylperoxo complexes.[39] In the referred paper, the authors suggested that acylperoxo complexes could exist in the so-called cis-β-configuration. To form the cis-β-configuration one of the oxygen atoms of the salen ligand has to leave the

basal plane creating two cis empty seats for coordination of acylperoxo ligand. However, this suggestion did not get further development in the literature.[1−3,11,14−22] The only exception is the highly relevant study on the mechanism of (Salen)Ti-catalyzed enantioselective sulfoxidation by hydrogen peroxide, where the authors prove the existence of cis-β-peroxo complex.[40,41]

There have been very few attempts to assess the O−O bond cleavage transformations in the acylperoxo complexes, despite its fundamental importance for understanding the reaction mechanism.[34−38] These experimental efforts are limited due to the transient nature of the reactive species and, therefore, are equivocal.
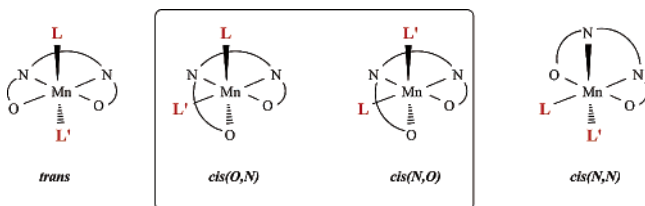
Hence, in the present paper, we perform density functional computational study to clarify the structural and electronic features of various acylperoxo complexes of (Salen)Mn-derivatives, and to investigate the O−O bond cleavage in these complexes to aid in the understanding of the mechanism of the oxygenation by (Salen)Mn systems.

II. Computational Methods

All calculations were performed with the Gaussian98 (G98) program suite.[42] For the present study, we used density functional theory (DFT), in particular, Becke's three-parameter hybrid exchange functional (B3)[43,44] combined with Lee−Yang−Parr's (LYP) correlation functional,[45] known as B3LYP. In a few cases (see below), for comparison with the B3LYP, we also used the nonhybrid BPW91 method containing the Becke88 exchange (B)[43] and Perdew−Wang's gradient corrected correlation (PW91) functionals.[46] Throughout this work, we used double-ζ LANL2DZ (D95V[47]) basis set with associated Hay−Wadt nonrelativistic effective core potential (ECP) on the Mn.[48,49] All geometries have been fully optimized without any symmetry constraints at the unrestricted B3LYP/LANL2DZ level. Vibrational frequency calculations have been performed only for the transition states to confirm the imaginary frequency. Therefore, the energy values used hereafter are without zero-point energy correction. Canonical Kohn−Sham orbitals have been visualized using Molden 3.6[50] and MOLEKEL 4.2.[51] To locate minima on the seams of crossing we used our own code SEAM[52,53] interfaced with HONDO95[54] and G98.

(14) Yamada, T.; Imagawa, K.; Nagata, T.; Mukaiyama, T. *Chem. Lett.* **1992**, 2231−2234.
(15) Yamada, T.; Imagawa, K.; Mukaiyama, T. *Chem. Lett.* **1992**, 2109−2112.
(16) Mukaiyama, T.; Yamada, T.; Nagata, T.; Imagawa, K. *Chem. Lett.* **1993**, 327−330.
(17) Imagawa, K.; Nagata, T.; Yamada, T.; Mukaiyama, T. *Chem. Lett.* **1994**, 527−530.
(18) Nagata, T.; Imagawa, K.; Yamada, T.; Mukaiyama, T. *Inorg. Chim. Acta* **1994**, *220*, 283−287.
(19) Yamada, T.; Imagawa, K.; Nagata, T.; Mukaiyama, T. *Bull. Chem. Soc. Jpn.* **1994**, *67*, 2248−2256.
(20) Nagata, T.; Imagawa, K.; Yamada, T.; Mukaiyama, T. *Bull. Chem. Soc. Jpn.* **1995**, *68*, 3241−3246.
(21) Imagawa, K.; Nagata, T.; Yamada, T.; Mukaiyama, T. *Chem. Lett.* **1995**, 335−336.
(22) Nagata, T.; Imagawa, K.; Yamada, T.; Mukaiyama, T. *Bull. Chem. Soc. Jpn.* **1995**, *68*, 1455−1465.
(23) Groves, J. T.; Watanabe, Y.; McMurry, T. J. *J. Am. Chem. Soc.* **1983**, *105*, 4489−4490.
(24) Groves, J. T.; Watanabe, Y. *J. Am. Chem. Soc.* **1986**, *108*, 7836−7837.
(25) Groves, J. T.; Watanabe, Y. *Inorg. Chem.* **1987**, *26*, 785−786.
(26) Groves, J. T.; Watanabe, Y. *J. Am. Chem. Soc.* **1986**, *108*, 7834−7836.
(27) Groves, J. T.; Watanabe, Y. *Inorg. Chem.* **1986**, *25*, 4808−4810.
(28) Groves, J. T.; Watanabe, Y. *J. Am. Chem. Soc.* **1988**, *110*, 8443−8452.
(29) Watanabe, Y.; Yamaguchi, K.; Morishima, I.; Takehira, K.; Shimizu, M.; Hayakawa, T.; Orita, H. *Inorg. Chem.* **1991**, *30*, 2581−2582.
(30) Yamaguchi, K.; Watanabe, Y.; Morishima, I. *Inorg. Chem.* **1992**, *31*, 156−157.
(31) Yamaguchi, K.; Watanabe, Y.; Morishima, I. *J. Chem. Soc., Chem. Commun.* **1992**, 1709−1710.
(32) Yamaguchi, K.; Watanabe, Y.; Morishima, I. *J. Am. Chem. Soc.* **1993**, *115*, 4058−4065.
(33) Machii, K.; Watanabe, Y.; Morishima, I. *J. Am. Chem. Soc.* **1995**, *117*, 6691−6697.
(34) Bryliakov, K. P.; Babushkin, D. E.; Talsi, E. P. *Mendeleev Commun.* **2000**, *1*, 1−3.
(35) Bryliakov, K. P.; Babushkin, D. E.; Talsi, E. P. *J. Mol. Catal. A: Chem.* **2000**, *158*, 19−35.
(36) Bryliakov, K. P.; Khavrutskii, I. V.; Talsi, E. P.; Kholdeeva, O. A. *React. Kinet. Catal. Lett.* **2000**, *71*, 183−191.
(37) Bryliakov, K. P.; Kholdeeva, O. A.; Vanina, M. P.; Talsi, E. P. *J. Mol. Catal. A: Chem.* **2002**, *178*, 47−53.
(38) Campbell, K. A.; Lashley, M. R.; Wyatt, J. K.; Nantz, M. H.; Britt, R. D. *J. Am. Chem. Soc.* **2001**, *123*, 5710−5719.
(39) Suzuki, M.; Ishikawa, T.; Harada, A.; Ohba, S.; Sakamoto, M.; Nishida, Y. *Polyhedron* **1997**, *16*, 2553−2561.

(40) Saito, B.; Katsuki, T. *Tetrahedron Lett.* **2001**, *42*, 3873−3876.
(41) Saito, B.; Katsuki, T. *Tetrahedron Lett.* **2001**, *42*, 8333−8336.
(42) Frisch, M. J.; Trucks, G. W.; Schlegel, H. B.; Scuseria, G. E.; Robb, M. A.; Cheeseman, J. R.; Zakrzewski, V. G., Jr.; J. A. M.; Stratmann, R. E.; Burant, J. C.; Dapprich, S.; Millam, J. M.; Daniels, A. D.; Kudin, K. N.; Strain, M. C.; Farkas, O.; Tomasi, J.; Barone, V.; Cossi, M.; Cammi, R.; Mennucci, B.; Pomelli, C.; Adamo, C.; Clifford, S.; Ochterski, J.; Petersson, G. A.; Ayala, P. Y.; Cui, Q.; Morokuma, K.; Malick, D. K.; Rabuck, A. D.; Raghavachari, K.; Foresman, J. B.; Cioslowski, J.; Ortiz, J. V.; Baboul, A. G.; Stefanov, B. B.; Liu, G.; Liashenko, A.; Piskorz, P.; Komaromi, I.; Gomperts, R.; Martin, R. L.; Fox, D. J.; Keith, T.; Al-Laham, M. A.; Peng, C. Y.; Nanayakkara, A.; Gonzalez, C.; Challacombe, M.; Gill, P. M. W.; Johnson, B. G.; Chen, W.; Wong, M. W.; Andres, J. L.; Head-Gordon, M.; Replogle, E. S.; Pople, J. A.; Revision A.6 ed.; Gaussian, Inc.: Pittsburgh, PA, 1998.
(43) Becke, A. D. *Phys. Rev. A: At., Mol., Opt. Phys.* **1988**, *38*, 3098−3100.
(44) Becke, A. D. *J. Chem. Phys.* **1993**, *98*, 5648−5652.
(45) Lee, C.; Yang, W.; Parr, R. G. *Phys. Rev. B: Condens. Matter Mater. Phys.* **1988**, *37*, 785.
(46) Perdew, J. P.; Chevary, J. A.; Vosko, S. H.; Jackson, K. A.; Pederson, M. R.; Fiolhais, C. *Phys. Rev. B: Condens. Matter Mater. Phys.* **1992**, *46*, 6671−6687.
(47) Dunning, T. H.; Hay, P. J. In *Mod. Theor. Chem.*; Schaefer, H. F., III, Ed.; Plenum: New York, 1977; Vol. 3, pp 1−27.
(48) Hay, P. J.; Wadt, W. R. *J. Chem. Phys.* **1985**, *82*, 270−283.
(49) Hay, P. J.; Wadt, W. R. *J. Chem. Phys.* **1985**, *85*, 299−310.
(50) Schaftenaar, G.; Noordik, J. H. *J. Comput.-Aided Mol. Design* **2000**, *14*, 123−134.
(51) Flükiger, P.; Lüthi, H. P.; Portmann, S.; Weber, J., 4.2 ed.; Swiss Center for Scientific Computing: Manno, Switzerland, 2000.
(52) Dunn, K. M.; Morokuma, K. *J. Chem. Phys.* **1995**, *102*, 4904−4908.
(53) Cui, Q.; Morokuma, K. *Chem. Phys. Lett.* **1996**, *263*, 54−62.
(54) Dupius, M.; Marquez, A.; Davidson, E. R., 6 ed.; IBM Corporation: Kingston, NY, 1995.

**Scheme 1.** Possible Configurations of the Octahedral Complexes of Mn(Salen)LL'. (see refs 39 and 55)

Scheme 2. Schematic Representation of the Four Isomers of Acylperoxo Complexes **2** and **3** Studied in This Paper

III. Results and Discussion

Throughout the paper, we label the complexes as $^{2S+1}A-X-$ ***info***, where **A** is the state symmetry, **2S+1** is the multiplicity, and **X** is **1** for the parent $[(Salen)Mn^{III}]^+$ complex, **2** for neutral $[(Salen)Mn^{III}(RCO_3)]$ and **3** for cationic $[(Salen)Mn^{IV}(RCO_3)]^+$ acylperoxo complexes. The rest of the label, ***info***, shows structural information (vide infra).

1. Geometrical Features of the Acylperoxo Complexes. We recognize that under the reaction conditions acylperoxo complexes can be formed by interaction of the $[(Salen)Mn^{III}]^+$ (**1**) with either acylperoxo anion (RCO_3^-) or radical $(RCO_3^{\bullet})$,[13] leading to neutral $[(Salen)Mn^{III}(RCO_3)]$ (**2**) and cationic $[(Salen)Mn^{IV}(RCO_3)]^+$ (**3**) complexes, respectively. In the literature, the structural diversity of the complexes of Mn with the tetradentate Schiff base ligands have been systematically reviewed, and several possible isomers, with **L** and/or **L'** ligands, have been proposed,[55,39] as depicted in Scheme 1. As the acylperoxo ligand can coordinate in either bidentate or monodentate mode to **1** to form octahedral or square pyramidal complexes, respectively, its actual coordination mode constitutes a question to be investigated.

Furthermore, it might be conceivable that the O−O fragment of the acylperoxo ligand could coordinate to the manganese in η^2 as opposed to η^1 mode, thus possibly resulting in some highly unusual 7-coordinate complexes of manganese. If such coordination mode is feasible, then unbiased geometry optimization should have been able to confirm it. However, we could not find any structure with η^2-coordinated O−O fragment. Besides, only few examples of O−O fragment coordinated to Mn are known from the literature.[56−58] Among those, two examples are available of peroxide O_2^{2-} and one of alkyl peroxide more relevant to our study. It is noteworthy that in former cases the complexes are 6-coordinate η^2, while in the latter case the complex is 4-coordinate η^1.

In the Scheme 1, the **trans** isomer represents a conventional unperturbed (Salen)MnLL' complex (where the three metalocycles lie in the same plane), whereas the **cis** isomers represent singly (with one of the three metalocycles perpendicular to the others, ***cis(O,N)*** and ***cis(N,O)***) and doubly perturbed (with each of the three metalocycles perpendicular to one another, ***cis(N,N)***) acylperoxo complexes. In the notation of the ***cis(Y,Z)*** isomers, **Y** and **Z** are the atoms of the Salen ligand, situated trans to the **L** and **L'** positions, respectively.
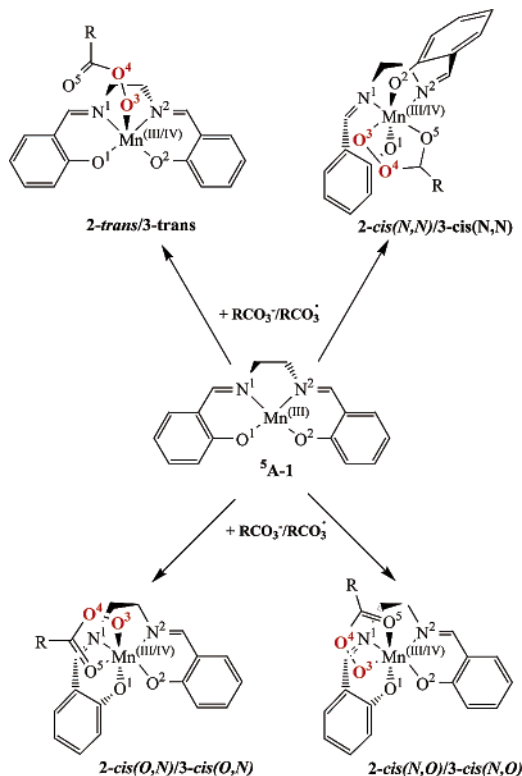
From the analysis presented above, it follows that our further discussion should consider one 5-coordinate ***trans-*** and three (***cis(O,N)***, ***cis(N,O)*** and ***cis(N,N)***) 6-coordinate ***cis*** acylperoxo complexes, as shown in Scheme 2. To determine geometric structures, ground electronic states, and relative energies of these four isomers of the complexes **2** and **3**, we have optimized their geometry within all plausible spin states.

The reference point for these calculations can be set at the quintet ground state of the reactant complex **1**,[38,59] with either acylperoxo anion (RCO_3^-) or radical $(RCO_3^{\bullet})$ for species **2** or **3**, respectively. We should note further that the gas-phase results obtained in this paper should be applicable to the aprotic nonpolar solvents such as benzene and toluene, where neither solvent−solute hydrogen bonding nor stabilization of ionic molecules are expected. Moreover in our calculations we did not consider the role of either axial ligands or hydrogen bonding interactions between the acylperoxo complexes and any hydrogen donor molecules. Work on these two effects on the structural properties of acylperoxo complexes and on the O−O bond cleavage will be published elsewhere.

From here, the paper is organized as follows: In Section **2**, we discuss electronic and geometric structures of the different isomers of complex $[(Salen)Mn^{III}(RCO_3)]$, **2**, whereas in the Section **3**, we discuss the cationic complex $[(Salen)Mn^{IV}-(RCO_3)]^+$, **3**. Section **4** is devoted to discussion of the mechanism of the O−O bond cleavage in complex **2** and **3**.

2. Neutral Acylperoxo Complex, $[(Salen)Mn^{III}(RCO_3)]$, 2. For the neutral complexes **2** possible spin states are quintet, triplet and singlet. Our B3LYP calculations show (Table 1) that the quintet state is the ground state for all studied isomers,

(55) Bermejo, M. R.; Fondo, M.; Garcia-Deibe, A.; Rey, M.; Sanmartin, J.; Sousa, A.; Watkinson, M.; McAuliffe, C. A.; Pritchard, R. G. *Polyhedron* **1996**, *15*, 4185−4194.

(56) VanAtta, R. B.; Strouse, C. E.; Hanson, L. K.; Valentine, J. S. *J. Am. Chem. Soc.* **1987**, *109*, 1425−1434.

(57) Kitajima, N.; Komatsuzaki, H.; Hikichi, S.; Osawa, M.; Moro-oka, Y. *J. Am. Chem. Soc.* **1994**, *116*, 11 596−11 597.

(58) Komatsuzaki, H.; Sakamoto, N.; Satoh, M.; Hikichi, S.; Akita, M.; Moro-oka, Y. *Inorg. Chem.* **1998**, *37*, 6554−6555.

(59) Bryliakov, K. P.; Babushkin, D. E.; Talsi, E. P. *Mendeleev Commun.* **1999**, *1*, 29−32.

Scheme 3. Energy Profile for the O−O Cleavage Transformations for the **2-*cis(O,N)***, **2-*cis(N,O)*** and **2-*trans*** Isomers of the Acylperoxo Complexes **2** (Solid Lines for Quintet and Dashed Lines for Triplet)
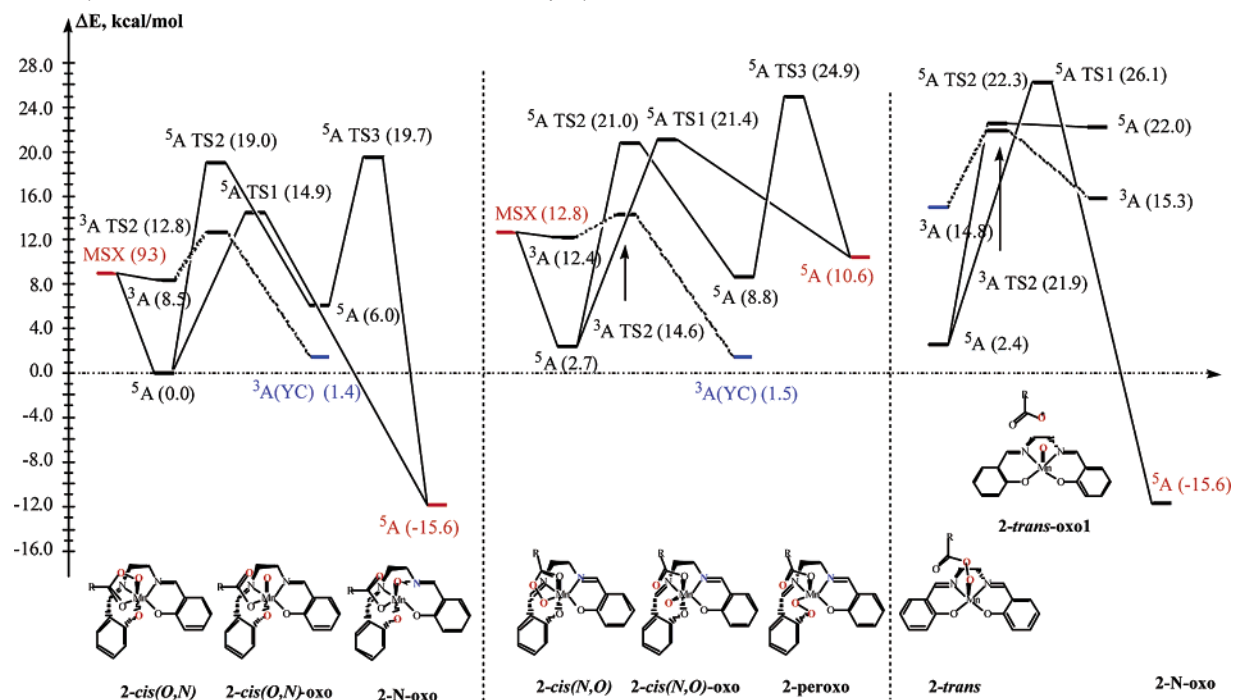

Table 1. Relative Energies E (in kcal/mol, relative to the **⁵A-2-*cis(O,N)*** for 2, and **⁴A-3-*cis(N,O)*** for 3) and <S²> Values for All Species in the Present Study[a]

species	state	trans		cis(O,N)		cis(N,O)		cis(N,N)	
		<S²>	E	<S²>	E	<S²>	E	<S²>	E
				acylperoxo complexes					
2	**⁵A**	6.05	2.4	6.05 (6.05)	0.0 (0.0)	6.05 (6.05)	2.7 (1.4)	6.08	16.7
	³A	2.05	14.8	2.02 (2.04)	8.5 (0.0)	2.02 (2.05)	12.4 (2.2)	2.02	20.9
	¹A(U)	0.97	25.3	1.06 (0.97)	19.1 (8.1)	1.02 (1.05)	24.2 (12.2)	1.01	32.5
	¹A(R)	-	34.5		30.3(12.8)		35.7 (19.7)	-	48.9
3	**⁴A**	4.03	6.9	3.80 (3.78)	0.5 (0.4)	3.81 (3.79)	0.0 (0.0)	3.85	20.6
	²A	1.58	23.5	1.65 (1.54)	13.5 (14.6)	1.80 (1.76)	15.9 (13.8)	1.44	29.2
				transition states, products and MSXs					
2-TS1	**⁵A**	6.05	26.1	6.05	14.9	6.06	21.4		
2-TS2	**⁵A**	6.10	22.3	6.18	19.0	6.18	21.0		
	³A	2.36	21.9	2.19	12.8	2.13	14.6		
2-TS3	**⁵A**			6.11	19.7	6.71	24.9		
2-insrt[b]	**⁵A**	6.06	−15.6	6.06	−11.8	6.06	10.6		
2-oxo[c]	**⁵A**	6.07[6.05]	22.0[−2.9]	6.05	6.0	6.04	8.8		
	³A(YC)	2.00[2.00]	15.3[−4.2]	2.00	1.4	2.00	1.5		
MSX	**⁵A/3A**			2.02/6.04	9.3	2.03/6.04	12.8		

[a] BPW91 relative energies where available are shown in parentheses. [b] **2-insrt** corresponds to the products of **TS1**; they are in the *trans* column **2-N-oxo(TB)**; in the *cis(O,N)* column, **2-N-oxo(SP)**. Note that either of the two products can form from either *trans* or *cis(O,N)*; and in the *cis(N,O)* column, **2-peroxo** product. [c] In the column *trans* in square brackets we provided the data for **2-trans-oxo2** species.

namely **2-*cis(O,N)***, **2-*cis(N,O)***, **2-*trans*** and **2-*cis(N,N)***. The isomer **2-*cis(O,N)*** is found to be the lowest in energy, with **2-*cis(N,O)***, **2-*trans***, and **2-*cis(N,N)*** isomers lying by 2.7, 2.4, and 16.7 kcal/mol higher, respectively. Corresponding triplet and highly spin-contaminated unrestricted singlet states (U) lie by 8.5, 9.7, 12.4, 4.2, and 19.1, 21.5, 22.9, 15.8 kcal/mol higher, relative to the quintet states of **2-*cis(O,N)***, **2-*cis(N,O)***, **2-*trans*** and **2-*cis(N,N)***, respectively. Noteworthy, restricted (R) singlet spin states are 30.3, 33.0, 32.1, and 32.2 kcal/mol higher than their quintet states, respectively.

For comparison with B3LYP, we provide selected energies obtained with the pure density functional BPW91 in parentheses in Table 1.[60] As seen from Table 1, BPW91 stabilizes low spin states by 8.5−12.0 kcal/mol relative to the hybrid B3LYP,

rendering quintet and triplet states of the isomers **2-*cis(O,N)*** and **2-*cis(N,O)*** nearly degenerate in energy. Regrettably, high level calculations (such as CCSD(T) and MRD-CI) to accurately

(60) The mentioned energy differences between the quintet, triplet and singlet states of the various isomers of the complex **2** have been obtained with the hybrid density functional, namely B3LYP, the accuracy of which, has been a subject of numerous investigations in the literature. (Khavrutskii, I. V.; Musaev, D. G.; Morokuma, K. *Inorg. Chem.* **2003**, *42*, 2606−2621; Abashkin, Y. G.; Collins, J. R.; Burt, S. K. *Inorg. Chem.* **2001**, *40*, 4040−4048; Brandt, P.; Norrby, P.-O.; Daly, A. M.; Gilheany, D. G. *Chem.-Eur. J.* **2002**, *8*, 4299−4307; Reiher, M.; Salomon, O.; Hess, B. A. *Theor. Chem. Acc.* **2001**, *107*, 48−55) It is suspected that the hybrid B3LYP functional may overestimate energies of the low spin states, due to the Hartree−Fock contribution in the Becke's three parameter exchange functional (B3). Therefore, to estimate possible error margins in the referred energy splittings, we have performed single point energy calculations for the isomers **2-*cis(O,N)*** and **2-*cis(N,O)*** with nonhybrid BPW91 functional. In these calculations we used the geometries optimized at the B3LYP level.

Table 2. Selected Geometrical Parameters (bonds in Å and angles in degrees) of Important Acylperoxo Complexes, Transition States, Products, and MSX Structures

species	state	Mn–O^2	Mn–O^1	Mn–N^1	Mn–N^2	Mn–O^3	Mn–O^5	<Mn–L>	O^3-O^4	R_{insrt}^{a}	O–(CH)	O^1–Mn–N^2	N^1–Mn–O^2	θ_{insrt}^{b}
						acylperoxo complexes								
2-trans	^{5}A	1.88	1.89	1.99	2.02	2.03	3.91	1.96	1.49	2.71	2.26	160.5	163.8	84.0
	^{3}A	1.86	1.87	1.98	1.99	1.84	3.67	1.91	1.50	2.67	3.85	161.1	166.8	88.2
	^{1}A(U)	1.86	1.87	1.98	1.99	1.83	3.65	1.91	1.50	2.67	3.94	157.3	165.5	88.8
	^{1}A(R)	1.90	1.83	2.02	1.92	1.79	3.44	1.89	1.51	2.82	4.55	132.9	173.8	98.8
2-cis(O,N)	^{5}A	1.87	1.93	2.01	2.15	2.06	2.29	2.05	1.50	2.61		121.4	166.8	76.8
	^{3}A	1.93	1.88	1.99	1.95	1.95	2.03	1.96	1.51	2.65		102.6	175.4	85.4
	^{1}(U)	1.91	1.90	1.99	1.96	1.94	2.04	1.96	1.51	2.65		102.9	174.9	85.9
	^{1}(R)	1.88	1.90	2.04	1.94	1.83	2.11	1.95	1.54	2.71		104.7	174.5	91.8
2-cis(N,O)	^{5}A	1.88	2.03	1.99	2.05	2.00	2.38	2.06	1.49	2.70		115.9	170.1	84.1
	^{3}A	1.88	1.92	1.98	2.01	1.91	2.05	1.96	1.53	2.66		95.4	171.6	88.0
	^{1}(U)	1.87	1.93	1.98	2.01	1.90	2.05	1.96	1.53	2.66		96.0	171.3	87.9
	^{1}(R)	1.89	1.88	2.04	1.97	1.83	2.21	1.97	1.54	2.76		111.5	169.0	95.9
2-cis(N,N)	^{5}A	1.92	1.91	2.26	2.11	1.96	2.32	2.08	1.49			98.8	114.9	
	^{3}A	1.92	1.91	1.99	2.04	1.90	2.03	1.97	1.53			99.0	103.0	
	^{1}A(U)	1.92	1.91	1.99	2.03	1.89	2.03	1.96	1.53			99.6	103.2	
	^{1}A(R)	1.94	1.88	1.97	1.99	1.88	2.04	1.95	1.53			104.3	102.8	
3-trans	^{4}A	1.84	1.82	1.98	1.98	1.88	3.76	1.90	1.46	2.71	2.38	160.5	162.4	89.2
	^{2}A	1.84	1.87	1.98	1.97	1.83	3.48	1.90	1.49	2.62	3.73	162.1	166.3	87.4
3-cis(O,N)	^{4}A	1.84	1.82	1.98	1.98	1.91	2.04	1.93	1.49	2.65		102.7	172.4	86.0
	^{2}A	1.98	1.85	1.96	1.96	1.93	2.01	1.95	1.50	2.60		104.8	173.8	83.8
3-cis(N,O)	^{4}A	1.83	1.84	1.98	1.95	1.95	1.99	1.92	1.50	2.56		101.0	170.7	86.8
	^{2}A	1.83	1.88	1.99	1.98	1.92	2.01	1.93	1.50	2.53		103.1	171.2	83.5
3-cis(N,N)	^{4}A	1.88	1.89	1.95	2.00	1.93	2.01	1.94	1.50			97.5	103.4	
	^{2}A	1.91	1.89	1.98	2.02	1.89	2.02	1.95	1.52			101.6	105.3	
						transition states and products								
2-trans-TS1	^{5}A	1.90	1.88	2.04	2.41	1.83	2.34	2.01	1.86	1.88	2.20	143.8	149.1	50.4
-TS2	^{5}A	1.87	1.86	1.98	1.99	1.73	4.00	1.88	2.01	2.70	2.22	158.2	163.9	92.7
	^{3}A	1.86	1.87	1.98	1.99	1.72	3.83	1.88	1.75	2.60	2.45	160.6	162.6	88.5
2-cis(O,N)-TS1	^{5}A	1.93	1.88	2.07	2.35	1.92	2.10	2.04	1.89	1.84		129.5	153.4	49.9
-TS2	^{5}A	1.87	1.97	1.99	2.01	1.89	2.08	1.97	1.87	2.50		114.3	168.4	79.4
	^{3}A	1.87	1.96	1.99	1.98	1.79	1.98	1.93	1.73	2.66		94.4	171.2	89.7
-TS3	^{5}A	1.89	1.90	1.99	2.04	1.87	1.90	1.93	3.23	1.72	2.68	116.1	167.0	52.1
2-cis(N,O)-TS1	^{5}A	1.92	2.30	2.08	2.03	1.87	2.09	2.05	2.09	1.77		128.2	161.8	49.0
-TS2	^{5}A	1.88	1.89	2.00	2.12	1.88	2.12	1.98	1.84	2.59		111.0	167.1	86.9
	^{3}A	1.88	1.92	1.99	2.04	1.78	2.01	1.94	1.71	2.65		93.0	171.1	91.5
-TS3	^{5}A	1.93	2.57	2.16	2.04	1.79	1.98	2.08	4.39	2.12	2.00	116.8	151.3	54.7
2-N-oxo(TB)	^{5}A	1.93	1.87	2.17	2.77	1.95	1.91	2.10	3.45	1.39	2.10		111.5	28.0
2-N-oxo(SP)	^{5}A	1.91	1.87	2.21	2.78	1.96	2.02	2.13	3.13	1.39	2.45		110.1	27.9
2-Peroxo	^{5}A	1.91	2.57	2.09	2.02	1.87	1.97	2.07	4.17	1.53	2.13		154.5	36.1
2-trans-oxo1	^{5}A	1.87	1.85	1.97	1.99	1.71	4.06	1.88	2.20	2.66	2.22	158.0	163.6	91.7
	^{3}A	1.87	1.85	1.97	2.00	1.68	3.98	1.87	2.10	2.69	2.19	157.1	161.2	93.7
2-trans-oxo2	^{5}A	1.87	1.88	1.97	1.99	1.81	1.95	1.91	5.02		2.16	173.7	173.5	
	^{3}A	1.88	1.87	1.99	2.00	1.81	1.93	1.91	5.07		2.14	172.5	174.0	
2-cis(O,N)-oxo	^{5}A	1.89	1.92	1.98	1.99	1.83	1.87	1.91	3.06	2.41	3.12	103.4	167.1	78.0
	^{3}A	1.88	1.95	1.98	2.01	1.77	1.89	1.91	2.34	2.57	3.35	96.3	168.3	85.4
2-cis(N,O)-oxo	^{5}A	1.89	1.88	2.00	2.05	1.80	1.91	1.92	2.40	2.44	3.90	102.1	168.5	83.1
	^{3}A	1.88	1.90	2.00	2.08	1.73	1.93	1.92	2.28	2.58	3.96	94.4	168.6	90.0
						minima on the seam of crossing								
MSX-cis(O,N)	^{5}A/^{3}A	1.92	1.90	2.00	2.00	1.98	2.08	1.98	1.51	2.67		105.0	173.9	84.5
MSX-cis(N,O)	^{5}A/^{3}A	1.88	1.94	1.99	2.02	1.93	2.08	1.97	1.52	2.66		96.9	170.9	87.0

^{a} R_{insrt} is the distance O^3–N^2 for **cis(O,N)** and **trans** isomers and O^3–O^1 for **cis(N,O)** isomer of acylperoxo complexes. ^{b} θ_{insrt} is the angle O^3–Mn–N^2 for **cis(O,N)** and **trans** and O^3–Mn–O^1 for **cis(N,O)** isomer of acylperoxo complexes.

describe the energetic order of the low-lying triplet and quintet states are practically impossible for such large systems. Therefore, we study two highest spin states, namely quintet and triplet, of all isomers of the complexes **2**, as well as their reactivity in greater details.

Because singlet states of all studied isomers, as well as all spin states of **cis(N,N)** are relatively high in energy, we narrow our discussion below to the triplet and quintet states of the **cis-(O,N)**, **cis(N,O)** and **trans** acylperoxo isomers.

As seen from Table 2, geometries corresponding to the same isomers in quintet and triplet states differ significantly. The most prominent difference between the quintet and triplet states for all three isomers is in the Mn–O^3 bond length, which is longer in the quintet state. Substantial elongations are also observed

in bonds Mn–N^2 and Mn–O^5, and Mn–O^1 and Mn–O^5, for quintet state of isomers **cis(O,N)** and **cis(N,O)**, respectively. Furthermore, for **cis** isomers in the quintet state the salen ligand appreciably deviates from pure octahedral geometry. In addition, for the **trans** isomer, a weak hydrogen bond between carbonyl oxygen and the ethylene bridge (O^5–(CH)), exists in the quintet state, but is absent in the triplet state. We believe that this feature is not significant because the hydrogen bond is on the order of 1 kcal/mol in the quintet state. Furthermore, as noted above, we do not consider hydrogen bonding interactions with the protic polar solvent molecules, which could easily destroy this weak interaction. The major geometrical differences between high and low spin states can be rationalized as follows; in the quintet state one of the four unpaired electrons occupies d$_{z^2}$-like orbital,

positioned along the most elongated bonds, while in the triplet state the d_{z^2}-like orbital is vacant, and the four electrons occupy only d_π orbitals. Therefore, we may conclude that the elongation of the bond distances, as well as change in the angles, observed in quintet states is due to repulsion between unpaired electron in the d_{z^2} orbital and corresponding ligand atoms.

3. Cationic Acylperoxo Complex, $[(Salen)Mn^{IV}(RCO_3)]^+$, 3. In the case of cationic complexes **3**, the available spin states are doublet and quartet. Our calculations demonstrate that the quartet state is the ground state for all studied isomers, namely **3-cis(O,N)**, **3-cis(N,O)**, **3-trans** and **3-cis(N,N)** (see Table 1). Unlike in the neutral complex, the lowest isomer is found to be **3-cis(N,O)**, with isomers **3-cis(O,N)**, **3-trans** and **3-cis(N,N)** lying 0.5, 6.9 and 20.6 kcal/mol higher in their quartet ground states, respectively. Corresponding doublet states are highly spin contaminated and lie by 15.9, 13.0, 16.6, and 8.6 kcal/mol higher, with respect to their quartet states. Surprisingly, both nonhybrid BPW91 and hybrid B3LYP functionals predict similar quartet-doublet energy differences for the isomers **3-cis(O,N)** and **3-cis(N,O)**, as opposed to quintet-triplet energy differences for species **2**.[60] As in the case with complex **2**, the isomer **3-cis-(N,N)** is substantially higher in energy than the other isomers, and thus is not discussed in detail here. We rationalize the energy difference between various isomers of complexes **2** and **3** based on the deformation energies of the salen molecule.[61]

Unlike in the complexes **2**, the difference in the inner-sphere metal−ligand distances between high (quartet) and low (doublet) state of complexes **3** is negligible, as seen in Table 2. Furthermore, angles of both quartet and doublet spin complexes are close to octahedral. Also in **3-trans** complexes the weak hydrogen bond, described earlier for the **2-trans** complexes is present in the quartet state but absent in the doublet state. Such small difference in the bond lengths, and angles between complexes in high and low spin states, compared to neutral **2** can be explained by the fact that in the quartet and doublet states of these isomers of **3** the unpaired electrons occupy exclusively d_π orbitals.

In brief, the observed difference in geometries between acylperoxo complexes **2** and **3** is due to the presence of extra electron in the species **2** relative to **3**, which populates the d_{z^2}-like orbital in the quintet ground state of **2**. This, in turn, causes substantial elongation of the metal−ligand bonds and deviation of the bond angles from pure octahedral symmetry in the quintet state of **2**, relative to complexes where the d_{z^2}-like orbital is empty, namely low spin states of **2** and both spin states of **3**. Therefore, low spin **2** and both spin states of **3** are very similar in geometry, with the minor exception of **trans** isomers where some deviation is observed in the weak hydrogen bond of dangling carbonyl oxygen with the ethylene bridge.

It is worth noting that whether you start with acylperoxo radical or anion, in the final complexes the acylperoxo ligand

appears as anion judging from the spin densities on Mn and O^3 atoms (see Table 2S of the Supporting Information), which indicate that Mn has about 4 unpaired electrons (Mn^{III}) in the quintet **2** and about 3 unpaired electrons (Mn^{IV}) in the quartet **3**, while corresponding O^3 atom carries at most 0.20e of spin in the **2-trans** and **3-trans**, but only 0.06e of spin in the **2-cis** and **3-cis** isomers of acylperoxo complexes. This requires one-electron intramolecular oxidation of the metal in cationic acylperoxo complexes.

Having characterized the geometric structures and relative energies of various acylperoxo complexes **2** and **3** we are now in a position to explore the O−O bond cleavage in these complexes.

4. General Comments on Mechanism of O−O Bond Cleavage in $[(Salen)Mn^{III}(RCO_3)]$, 2. As noted in the Introduction, acylperoxo complexes are commonly believed to display dual nature in the oxidation reactions,[26−33] acting either independently or producing other reactive species via the O−O bond cleavage. However, very little is known about the nature and factors controlling such transformations of acylperoxo complexes, due to their transient character. Therefore, we decided to address these issues using quantum chemical methods. Below, we report our rigorous study of the mechanism of the O−O bond cleavage in the acylperoxo complexes **2** and **3** in the absence of extra ligands. Note that aprotic solvents, such as acetonitrile, benzene, toluene, and dichloromethane, are usually used as reaction media.[1,2,5−8,11,17,62] As we mentioned earlier, we expect that the results obtained here will be relevant to aprotic nonpolar solvents (benzene, toluene, etc.), whereas in polar solvents (acetonitrile, dichloromethane, etc.) stabilization of ionic molecules may possibly change the mode of O−O cleavage from homolytic to heterolytic.

We first discuss the mechanism of the O−O bond cleavage in neutral acylperoxo complex $[(Salen)Mn^{III}(RCO_3)]$, **2**. Here, we consider the O−O bond cleavage for the quintet and triplet states of the **cis(O,N)**, **cis(N,O)** and **trans** isomers of **2**. As mentioned previously, due to their high energies, we completely exclude **cis(N,N)** isomer,[61] as well as singlet states of all other isomers from our study. In principle, the O−O bond cleavage can proceed with and without intramolecular insertion, consequently resulting in two different products. In the former case, intramolecular insertion occurs either into Mn−O or Mn−N bond with the Salen ligand, leading to peroxo or N-oxo species, respectively. The O−O bond cleavage without intramolecular insertion leads to various **oxo** species. Furthermore, we can qualitatively classify the O−O bond cleavages into heterolytic or homolytic by examining spin densities on the O^4 and O^5 (Table 2S) in the transition states and more importantly corresponding products. Whenever we see only a small fraction (tentatively less than 0.20) of a spin on O^4 and/or O^5 in the product, we conclude that the process is heterolytic. On the contrary, if we see significant fraction of a spin (tentatively larger than 0.50) on the referred atoms in the products, then we conclude that homolytic cleavage has occurred.

Because the O−O bond cleavage in the high (quintet) and low (triplet) spin states of the **cis(O,N)**, **cis(N,O)** and **trans** isomers could occur differently, it is worth discussing these spin states separately.

5. O−O Bond Cleavage in the Quintet 2-cis(O,N), 2-cis-(N,O), and 2-trans Isomers. As seen in Figure 2 and Tables 1

(61) To better understand the nature of the (Salen)Mn-acylperoxo complexes, we have computed the deformation energy of the salen fragment from its ground quintet equilibrium structure to that in the complex. The results are summarized in the Table 5S of Supporting Materials. The data in the Table 5S confirm that **cis(N,N)** complexes are less stable than **cis(O,N)** and **cis(N,O)** complexes due to higher Salen deformation energy of the former. It also implies that interaction energy in **cis** complexes is substantially larger than in **trans**. Furthermore, entropy factors would prefer **cis** complexes to **trans** due to chelate bidentate coordination mode of the former. The only question that remains is whether such high deformation energies of the **cis** complexes are accessible during the reaction. To assess this question we performed relaxed potential energy surface scan from ^{5}A-2-**cis(O,N)** to ^{5}A-2-**trans** acylperoxo complex and estimated the barrier to be less than 6.0 kcal/mol.
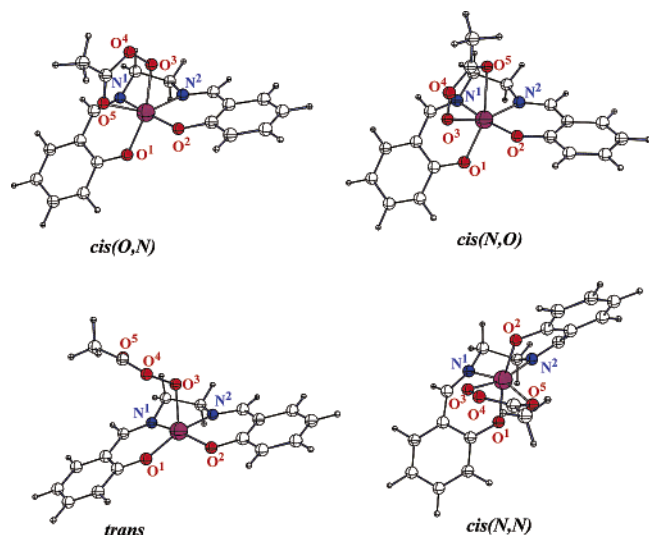
Figure 1. Optimized structures of the different isomers (*cis(O,N)*, *cis-(N,O)*, *trans* and *cis(N,N)*) of acylperoxo complexes **2** and **3**.

and 2S, in the quintet spin state of the isomer **2-cis(O,N)**, the O−O bond cleavage coupled with intramolecular insertion of the terminal peroxo oxygen (O^3) into the Mn−N^2 bond (**2-cis-(O,N)-TS1**) is heterolytic (spin densities on O^4 and O^5 are 0.02e and 0.07e in the TS1, and 0.02e and 0.04e in the lowest energy product, respectively) and proceeds with 14.9 kcal/mol barrier. As a product two isomeric **2-N-oxo** species can be formed (Figure 2) with manganese in the oxidation state III, the lowest of which is 15.6 kcal/mol below the reactant **2-cis(O,N)**. Note that in the literature the formation of analogous **N-oxo** species has been reported for Fe,[24,28,63] Ni,[64] and tentatively Mn[65,66] porphyrin complexes. Also the **N-oxo** porphyrin complexes of Fe[67] and Mn[68−70] have been studied theoretically. Noteworthy, pure O−O bond cleavage via **2-cis(O,N)-TS2** (see Figure 3) is also heterolytic (spin densities on O^4 and O^5 are 0.28e and 0.04e in the TS2, and only 0.03e and 0.12e in the final product, respectively), but surmounts a higher barrier of 19.0 kcal/mol. In this case, the product is unusual **2-cis(O,N)-oxo** species with manganese formally in the oxidation state V, and the reaction is 6.0 kcal/mol endothermic. Therefore, one may expect that major product of the O−O bond cleavage in quintet **2-cis(O,N)** would be quintet **2-N-oxo** species.

In the isomer **2-cis(N,O)**, the O−O bond cleavage with (via **2-cis(N,O)-TS1**) and without (via **2-cis(N,O)-TS2**) intramolecular insertion proceeds heterolytically (the spin densities on O^4 and O^5 atoms are −0.01e and 0.08e, 0.26e and 0.03e for TS1 and TS2, respectively, and 0.02e and 0.12e, and 0.15e and 0.05e for corresponding products) with almost identical barriers, 18.7 and 18.3 kcal/mol, respectively. The product of the intramolecular insertion pathway is **2-peroxo** complex (Mn^{III}),

(62) Jacobsen, E. N.; Deng, L.; Furukawa, Y.; Martinez, L. E. *Tetrahedron* **1994**, *50*, 4323−4334.
(63) Groves, J. T.; Nemo, T. E. *J. Am. Chem. Soc.* **1983**, *105*, 5786−5791.
(64) Balch, A. L.; Chan, Y.-W.; Olmstead, M. M. *J. Am. Chem. Soc.* **1985**, *107*, 6510−6514.
(65) Bortolini, O.; Meunier, B. *J. Chem. Soc., Chem. Commun.* **1983**, 1364−1366.
(66) Bortolini, O.; Ricci, M.; Meunier, B.; Friant, P.; Ascone, I.; Goulon, J. *Nouv. J. Chim.* **1986**, *10*, 39−49.
(67) Den Boer, D. H. W.; Van der Made, A. W.; Zwaans, R.; Van Lenthe, J. H. *Recl. Trav. Chim. Pays-Bas* **1990**, *109*, 123−126.
(68) Strich, A.; Veillard, A. *Nouv. J. Chim.* **1983**, *7*, 347−352.
(69) Jorgensen, K. A. *Acta Chem. Scand., Ser. B* **1986**, *40*, 512−514.
(70) Jorgensen, K. A. *J. Am. Chem. Soc.* **1987**, *109*, 698−705.

whereas the product of the pure O−O bond cleavage is another unusual **2-cis(N,O)-oxo** species (Mn^V), lying 7.9 and 6.1 kcal/mol above the **2-cis(N,O)**, respectively.

In the case of **trans** acylperoxo complexes, the O−O bond cleavage coupled with intramolecular insertion (**2-trans-TS1**) is also heterolytic (the spin densities on O^4 and O^5 atoms are 0.04e and 0.01e, and 0.02e and 0.04e for TS1 and corresponding lowest energy product, respectively), but surmounts a substantially higher barrier of 23.7 kcal/mol. This reaction provides an alternative path to the same **N-oxo** product, as in the case with **2-cis(O,N)**. Remarkably, unlike in the **cis** acylperoxo complexes, the pure O−O bond cleavage in the **trans** acylperoxo complexes via the transition state **2-trans-TS2** is homolytic (the spin densities on O^4 and O^5 atoms are 0.62e and 0.00e, and 0.65e and 0.00e for TS2 and corresponding product, respectively) and surmounts a 19.9 kcal/mol barrier. The resulting neutral (Salen)-Mn^{IV}(O) **2-trans-oxo1** species (Figure 3) has a carboxylate radical bound to the ethylene bridge through a weak hydrogen bond. Energetically **2-trans-oxo1** is only 0.3 kcal/mol lower than the **2-trans-TS2** and thus the reaction is 22.0 kcal/mol endothermic.

Finally, the question of isomerization between products of O−O bond cleavage with and without intramolecular insertion can be of some interest when stability of the resulting unusual Mn^V **cis-oxo** species is in question. We have performed transition state (**TS3**) search connecting **2-cis(O,N)-oxo** to **N-oxo**, and **2-cis(N,O)-oxo** to **peroxo** and found these processes to have barriers of 13.7 and 16.1 kcal/mol, respectively. Because **2-cis(O,N)-TS3** and **2-cis(N,O)-TS3** are of little interest, we do not discuss these transition states in detail here (details can be found in the Supporting Information).

Now, let us discuss the important geometrical parameters of the products of the O−O bond cleavage, **2-N-oxo**, **2-peroxo**, and **2-oxo** complexes, given in Figures 2 and 3, as well as in Table 2. We discuss the geometries of these products according to their energetic order.

In the case of the **2-N-oxo** species, we have located two distinct isomers with energy difference of 3.7 kcal/mol (see Table 1). The lowest isomer (called **2-N-oxo(TB)**) has a trigonal bipyramidal (TB) configuration, and contains a weak hydrogen bond between O^4 and the ethylene bridge. The other isomer (called **2-N-oxo(SP)**) does not contain the hydrogen bond because the carboxylate ligand is in the bidentate mode, resulting in more octahedral geometry.

To the best of our knowledge, the unusual Mn^V **cis-oxo** species have never been suggested in the literature, therefore we describe their features in more details here. The **2-cis(O,N)-oxo** and **2-cis(N,O)-oxo** species unlike their parent acylperoxo complexes have near octahedral structure. The O−O bond is completely broken (>2.4 Å), and the Mn−O^3 bond becomes 1.83 and 1.80 Å in the **2-cis(O,N)-oxo** and **2-cis(N,O)-oxo**, respectively. For comparison with these **cis-oxo** species we have optimized geometry of conventional Mn^V **oxo** species with carboxylate ligand positioned trans to the oxo ligand (called **2-trans-oxo2**), similar to that described in our previous paper.[71] This conventional **2-trans-oxo2** species has nearly flat arrangement of the salen coordination sphere around Mn atom, with Mn−O^3 bond of 1.81 Å perpendicular to that salen plane.

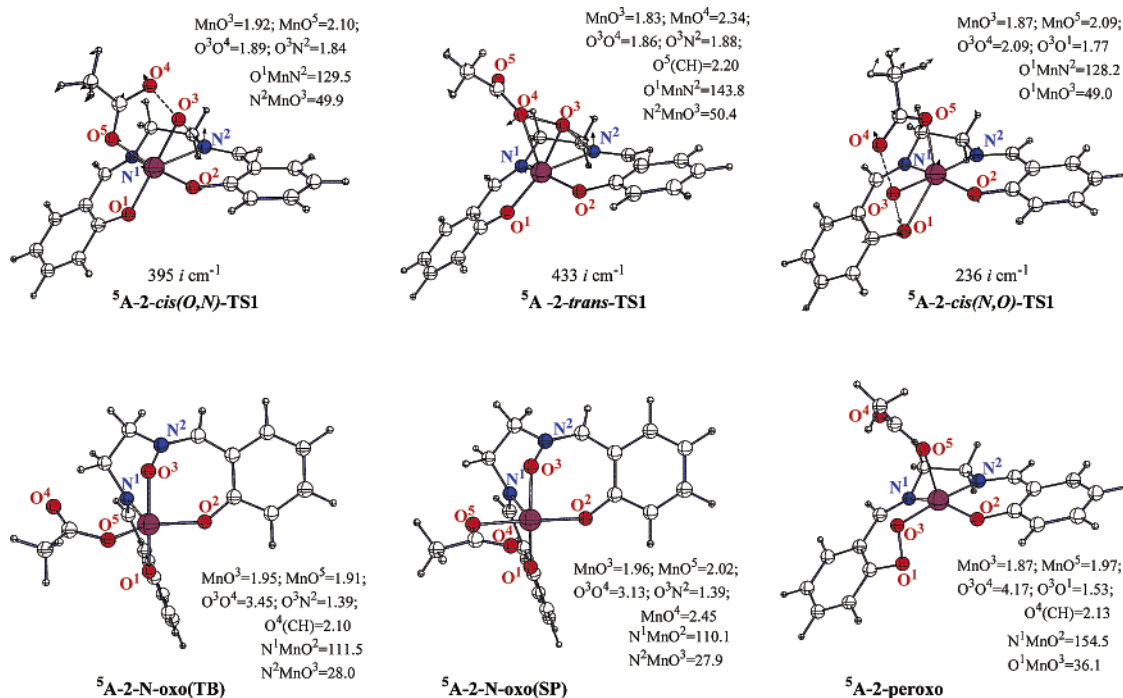(71) Khavrutskii, I. V.; Musaev, D. G.; Morokuma, K. *Inorg. Chem.* **2003**, *accepted*.

Figure 2. Transition states (**TS1**) and products of O—O bond cleavage coupled with intramolecular insertion in the quintet state in the different isomers of the acylperoxo complex **2**, and their important geometric parameters (distances in Å, angles in deg.).
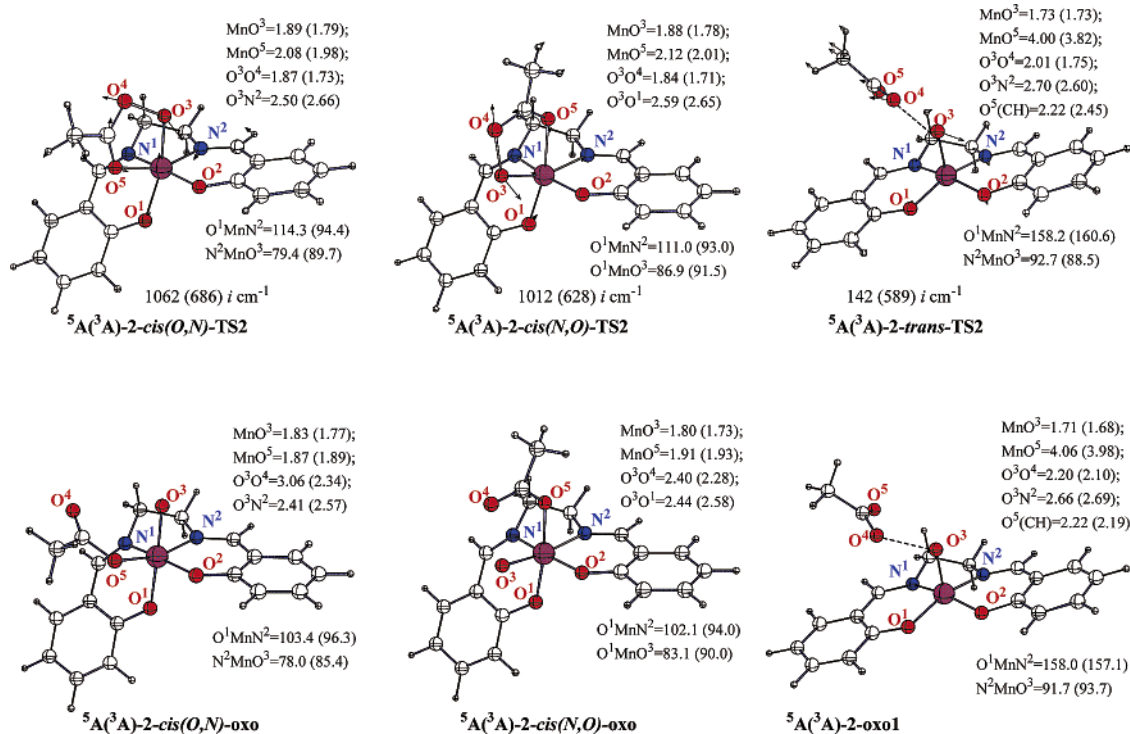

Figure 3. Transition states (**TS2**) and products of pure O—O bond cleavage in the quintet and triplet (in parentheses) spin states in the different isomers of the acylperoxo complex **2**, and their important geometric parameters (distances in Å, angles in deg).

Interestingly, as seen in Table 1, the **2-trans-oxo2** species is substantially lower in energy than the **2-cis(O,N)-oxo** and **2-cis-(N,O)-oxo**, species and is 2.9 kcal/mol below **2-cis(O,N)**, presumably due to less strain in the Salen ligand.

For the **2-peroxo**, we have found only one isomer with a square pyramidal configuration, which also contains a hydrogen bond between O^4 and the ethylene bridge. Due to the high

energy of this product, we believe that it does not contribute to the reaction.

The product of the O—O bond cleavage in the **2-trans** complex is a (Salen)Mn^{IV}(O) (**2-trans-oxo1**) species, with weakly bound carboxylate radical, ferromagnetically coupled with the three unpaired electrons of (Salen)Mn^{IV}(O) (see Table 2S in the Supporting Information). The presence of this radical

ligand in the inner sphere of the complex changes the $Mn-O^3$ bond length from 1.66 to 1.71 Å compared to (Salen)Mn^{IV}(O) in the ground quartet state.[71] We believe that Mn^{IV} **2-*trans*-oxo1** species can further isomerize with intramolecular electron transfer to Mn^V **2-*trans*-oxo2** species mentioned above.

In summary, the acylperoxo complexes in the quintet spin state may undergo heterolytic O—O bond cleavage coupled with intramolecular insertion, leading to fairly stable ***N*-oxo** species. Furthermore, with somewhat higher barriers the ***cis*** acylperoxo complexes can produce unusual intermediate Mn^V ***cis*-oxo** species through pure heterolytic O—O bond cleavage. Last, the ***trans*** acylperoxo complex can take a homolytic route to form (Salen)Mn^{IV}(O) species with weakly bound carboxyl radical, which can probably isomerize to a lower energy intermediate Mn^V **2-*trans*-oxo2** species. *The lowest in energy of all products, forming with the smallest barrier on the quintet spin surface, is the N-oxo species.*

6. O—O Bond Cleavage in the Triplet 2-*cis(O,N)*, 2-*cis*-(N,O) and 2-*trans* Isomers. Our calculations (see Figure 3, and Tables 1, 2 and 2S) show that the O—O bond cleavage in triplet *cis* acylperoxo isomers occurs in a different fashion than in their high spin analogues. First, it proceeds with low barriers of only 4.3 and 2.2 kcal/mol for **2-*cis(O,N)*** and **2-*cis(N,O)***, respectively. Second, the O—O bond cleavage in the low spin complexes **2-*cis(O,N)*** and **2-*cis(N,O)*** is completely uncoupled from intramolecular insertion (taking place via **TS2** using the notation in the preceding section) and, therefore, leads exclusively to **2-*cis(O,N)*-** and **2-*cis(N,O)*-oxo** species.[72] Such pure O—O bond cleavage is found to be heterolytic in the *cis* acylperoxo complexes (the spin densities on O^4 and O^5 are −0.15e and −0.01e, and −0.13e and −0.01e for *cis(O,N)*- and *cis(N,O)*-TS2, and −0.14e and −0.00e, and −0.18e and −0.02e for corresponding products, respectively). The corrected energies[72] of the unusual triplet **³A(YC)-2-*cis(O,N)*-** and **³A(YC)-2-*cis*-(N,O)-oxo** species are only 1.4 and 1.5 kcal/mol higher than the **⁵A-2-*cis(O,N)***, but 7.1 and 10.9 kcal/mol lower than reactants **³A-2-*cis(O,N)*** and **³A-2-*cis(N,O)***, respectively. Also note that the triplet states of the *cis*-2-oxo species, **³A(YC)-2-*cis(N,O)*-oxo** and **³A(YC)-2-*cis(N,O)*-oxo** are calculated to be 4.6 and 7.3 kcal/mol lower than **⁵A-2-*cis(O,N)*-oxo** and **⁵A-2-*cis(N,O)*-oxo**, respectively.

In the triplet **2-*trans*** isomer, the O—O bond cleavage (via **2-*trans*-TS2**) is very similar to the one in the quintet state. It is again homolytic (the spin densities on O^4 and O^5 are −0.34e and 0.00e, and −0.56e and 0.00e) and proceeds with smaller barrier of 7.2 kcal/mol. The product in this case is symmetry broken **³A-2-*trans*-oxo1** species with quartet (Salen)Mn^{IV}(O) anti-ferromagnetically coupled to carboxyl radical (the spin densities on Mn, O^3, and O^4 are calculated to be 2.64, −0.13,

and −0.56, respectively, implying that about three α electrons occupy the Mn atom, whereas about one β electron is shared between O^3 and O^4 atoms, with greater fraction located on O^4). The presence of this radical ligand in the inner sphere of the complex only slightly affects the $Mn-O^3$ bond length as opposed to the quintet case, changing it from 1.66 to 1.68 Å compared to (Salen)Mn^{IV}O in the ground quartet state.[71] After Yamaguchi correction[72] the energy of this product becomes 15.3 kcal/mol above the **⁵A-2-*cis(O,N)***. Similar to **⁵A-2-*trans*-oxo1**, in **³A-2-*trans*-oxo1** the carboxylate ligand has a driving force to migrate into the axial position to become **³A-2-*trans*-oxo2**, because the latter lies by 4.2 kcal/mol lower than **⁵A-2-*cis(O,N)***.

Geometrically the products of the pure O—O bond cleavage in the triplet state complexes are very similar to those in the quintet state. Therefore, we omit discussion of the structure of the products here.

To summarize, we stress that, unlike in the quintet acylperoxo complexes, in the triplet state the O—O bond cleavage is completely uncoupled from intramolecular insertion, and proceeds with substantially smaller barriers.

Interplay between Quintet and Triplet Pathways. So far, we have discussed the O—O bond cleavage paths in quintet and triplet acylperoxo complexes **2** separately, and showed that in the ground quintet state of acylperoxo complexes the O—O cleavages have high barriers, whereas in higher energy triplet acylperoxo complexes the O—O cleavage barriers are substantially lower. More precisely, we have demonstrated that in the ground quintet electronic states of **2-*cis(O,N)***, **2-*cis(N,O)*** and **2-*trans***, O—O bond cleavage may proceed via two distinct pathways, with (leading to **2-*N*-oxo** or **2-peroxo**) and without (leading to **2-oxo** species) intramolecular insertion which are calculated to have high activation barriers of 14.9, 18.7, and 23.7 and 19.0, 18.3 and 19.9 kcal/mol, respectively. The most stable intermediate resulting from these O—O bond cleavages is the ***N*-oxo** complex, which forms with the lowest barrier and lies 15.6 kcal/mol lower than most stable reactant **2-*cis(O,N)***. Therefore, one may expect that major product of the O—O bond cleavage in quintet state would be quintet **2-*N*-oxo** species.

Although the triplet states of the isomers **2-*cis(O,N)***, **2-*cis*-(N,O)** and **2-*trans***, are calculated to be 8.5, 9.7 and 12.4 kcal/mol higher relative to their quintet states, respectively, the O—O bond cleavage in these triplet isomers proceeds with significantly lower barriers (4.3, 2.2 and 7.2 kcal/mol for **2-*cis(O,N)***, **2-*cis*-(N,O)** and **2-*trans***, respectively) and is completely uncoupled from intramolecular insertion. The resulting oxo species, namely, **2-*cis(O,N)*-**, **2-*cis(N,O)*-oxo** and **2-*trans*-oxo1**, are 1.4, 1.5, and 15.3 kcal/mol[72] higher than the lowest quintet reactant **⁵A-2-*cis(O,N)***, but 7.1 and 10.9 kcal/mol lower than triplet reactants **³A-2-*cis(O,N)*** and **³A-2-*cis(N,O)***, respectively.

Thus, these data show that the promotion (from quintet to triplet states) plus O—O bond activation (calculated for the triplet isomers) energies are 12.8, 11.9, and 19.5 kcal/mol for the **2-*cis*-(O,N)***, **2-*cis(N,O)*** and **2-*trans***, respectively. These values are lower than the lowest O—O bond activation barriers, 14.9, 18.3 and 19.9 kcal/mol, within the quintet states for the **2-*cis(O,N)***, **2-*cis(N,O)*** and **2-*trans***, respectively. This may suggest alternative pathways for the transformation of the acylperoxo-complex **2**. In particular, transformation of the acylperoxo complex can start from the ground quintet states, proceed through the minima on the seam of crossing (MSXs) between the quintet and triplet

(72) The resulting **2-*cis(O,N)*-** and **2-*cis(N,O)*-oxo** complexes are highly spin contaminated (as seen from $<S^2>$ values in Table 2S and 4S, which are 2.91 and 2.85 for **2-*cis(O,N)*-** and **2-*cis(N,O)*-oxo**, respectively) due to symmetry-broken nature of the obtained UB3LYP solution. Thus, in this triplet complexes, the unpaired electrons are not just two α, but instead three α and one β (As seen from the Table 2S, where atoms Mn and O^3 carry 2.80 and −0.74 (in **2-*cis(O,N)*-oxo**), and 2.74 and −0.64 (in **2-*cis*-(N,O)-oxo**) of an electron, respectively. This is equivalent to say that there are about three unpaired α electrons on Mn atom, and one β electron on O^3). Therefore, the calculated energy of these complexes is corrupted by admixture of pure spin quintet solution. To approximate the energy of the pure ³A spin states, we applied the Yamaguchi correction scheme (Yamaguchi, K. *Chem. Phys. Lett.* **1988**, *149*, 537−542; Yamaguchi, K.; Fukui, H.; Fueno, T. *Chem. Lett.* **1986**, 625−628) as described in our previous paper. (Khavrutskii, I. V.; Musaev, D. G.; Morokuma, K. *Inorg. Chem.* **2003**, *42*, 2606−2621)

potential energy surfaces, and form triplet oxo species with overall a lower energy than the pathway on the quintet potential energy surface. The only problem that remains to be assessed is the energy of these crossing points between quintet and triplet potential energy surfaces (MSXs). Since the energy of the O−O bond cleavage in **2-trans** is higher than in **cis** acylperoxo complexes, we believe that **cis** acylperoxo complexes exclusively will determine the products of the O−O bond cleavage. Therefore, below, we discuss this alternative pathway, especially the minima on the seam of crossing (MSXs) between the quintet and triplet states of the **2-cis(O,N)** and **2-cis(N,O)** isomers, in more details.

7. Description of Seams of Crossing (MSXs) between Quintet and Triplet Species. We have located the minima on the seams of crossing (MSXs) between the quintet and triplet states of the **2-cis(O,N)** and **2-cis(N,O)** isomers, ^{3}A/^{5}A-2-cis-(O,N)-MSX and ^{3}A/^{5}A-2-cis(N,O)-MSX, respectively. The geometries of these MSXs resemble corresponding triplet acylperoxo complexes. The important geometrical parameters of these structures are provided in Table 2, whereas their full geometries are given in Table 1S of the Supporting Information. Their relative energies are included in Table 1. As seen in Table 1, ^{3}A/^{5}A-2-cis(O,N)-MSX and ^{3}A/^{5}A-2-cis(N,O)-MSX are only slightly, 0.8 and 0.4 kcal/mol, higher in energy than their corresponding triplet minima, ^{3}A-2-cis(O,N) and ^{3}A-2-cis(N,O), respectively, which make the alternative pathway feasible.

Thus, the present results allow us to conclude that the transformation of the energetically most favorable isomer **2-cis-(O,N)** of the acylperoxo complex **2** may proceed via two distinct pathways. First of them corresponds to the direct O−O bond activation on the quintet state surface leading to the **2-N-oxo** product. This reaction occurs with a 14.9 kcal/mol barrier and is 15.6 kcal/mol exothermic. Alternatively, starting from the quintet ground state the reaction could proceed through the minimum on the seam of crossing (MSX) between the quintet and triplet state potential energy surfaces followed by the O−O bond cleavage on the triplet surfaces. This would lead to the triplet Mn^V **2-cis(O,N)-oxo** species with only 12.8 kcal/mol of activation energy, calculated relative to quintet **2-cis(O,N)**, because the MSX between the quintet and triplet states is located before the quintet O−O activation transition state. The second pathway is endothermic by 1.4 kcal/mol, relative to the quintet **2-cis(O,N)**. Thus, the first pathway is thermodynamically more favorable than the second pathway. However, one may expect that the formation of Mn^V **2-cis(O,N)-oxo** would be kinetically slightly more favored than formation of **2-N-oxo** because the latter has an activation energy lower by about 2.0 kcal/mol. Similar conclusions could be made for the **2-cis(N,O)** isomer.

The above conclusions have been based on the results obtained at the hybrid B3LYP level. However, it is well-known (as discussed in subsection **2**) that the hybrid B3LYP functional tends to overestimate (in this case by 8.5−12.0 kcal/mol, relative to the pure density functional BPW91) the energies of low spin states. Therefore, one may expect that at the pure density functional level the less favorable quintet state pathway will be additionally destabilized, and our most favorable pathway occurring through the triplet reactants, transition states, and products will be additionally stabilized, which will further reduce the overall barrier for the formation of the Mn^V **cis-oxo** species.

To complete this section, we would like to point out that investigation of the mechanism of the O−O bond cleavage in acylperoxo complexes in the absence of the olefin substrate is an essential step toward understanding the epoxidation mechanism in the KJK system, because without such study no conclusion could be drawn concerning the involvement of any of the species discussed here in epoxidation. Currently, work on the epoxidation reaction by acylperoxo complexes **2** and **3** as well as by the products of their O−O cleavage is in progress and preliminary results indicate that O−O cleavage is likely to occur prior epoxidation. We do not reveal any numbers here because they will be published elsewhere, but we would like to point to an article on epoxidation by organic peracids that was published while this manuscript was in the referees' hands. The insights on the importance of the present paper can be derived from there.[73]

8. O−O Cleavage of [(Salen)Mn^{IV}(RCO$_3$)]$^+$, 3. Unlike neutral acylperoxo complex **2**, the transformation of its cationic counterpart **3** in both (quartet and doublet) spin states simply goes uphill in energy upon stretching the O−O bond. This can be rationalized on the basis of the electronic structure of species **3**. Among the LUMO orbitals the lowest one corresponds to O^3−O^4 σ* orbital (not shown). Thus, at least one extra electron is necessary to populate this orbital, and consequently to break the O^3−O^4 bond. Therefore, the cationic complexes **3** have to be activated by 1-electron reduction, which is very likely event in the oxidation conditions. In the absence of reducing agents the acylperoxo complex **3** would be unreactive toward O−O bond cleavage and should be experimentally observed for example by ESR techniques, possibly in three isomeric forms **3-cis(O,N)**, **3-cis(N,O)**, and **3-trans**.

IV. Conclusions

From the presented discussions one can draw the following conclusions:

1. Four isomers of the complexes [(Salen)Mn^{III}(RCO$_3$)], **2**, and [(Salen)Mn^{IV}(RCO$_3$)]$^+$, **3**, have been characterized, three of which (cis(O,N), cis(N,O) and cis(N,N)) have 6-coordinated **cis**, whereas one has 5-coordinated **trans**, structure. At the hybrid density functional (B3LYP) level, the ground electronic states of all isomers of **2**, namely **2-cis(O,N)**, **2-cis(N,O)**, **2-cis-(N,N)**, and **2-trans** are found to be quintet states. The isomer **2-cis(O,N)** is found to be the lowest in energy, with **2-trans**, **2-cis(N,O)** and **2-cis(N,N)** isomers lying by 2.4, 2.7, and 16.7 kcal/mol higher, respectively. The corresponding triplet states lie by 8.5, 12.4, 9.7, and 4.2 kcal/mol higher than the quintet states, respectively. The ground electronic states of the isomers of the complex **3** are found to be quartet states with doublet states lying significantly higher in energy. Energetically, nearly degenerate isomers **3-cis(O,N)** and **3-cis(N,O)** are found to be the lowest in energy.

2. Nonhybrid density functional BPW91 stabilizes low spin states of acylperoxo complex **2** by 8.5−12.0 kcal/mol relative to hybrid B3LYP, rendering quintet and triplet states of the isomers **2-cis(O,N)** and **2-cis(N,O)** nearly degenerate in energy. Surprisingly, both nonhybrid BPW91 and hybrid B3LYP functionals predict similar quartet-doublet energy differences for the isomers **3-cis(O,N)** and **3-cis(N,O)**.

(73) Bach, R. D.; Dmitrenko, O.; Adam, W.; Schambony, S. *J. Am. Chem. Soc.* **2003**, *125*, 924−934.

3. The results obtained at the hybrid DFT (B3LYP) level show that the transformation of the acylperoxo complex **2** may proceed via two distinct pathways. First of them corresponds to the direct O−O bond activation on the quintet state surface coupled with insertion of the oxygen into Mn−N(Salen) bond, and leads to **2-N-oxo** species. Alternatively, the transformation could proceed through the minimum on the seam of crossing (MSX) between the quintet and triplet states, followed by the pure heterolytic O−O bond cleavage on the triplet surface, and lead to the triplet Mn^V **2-cis-oxo** species. According to our calculations the first pathway is thermodynamically, while second pathway is kinetically slightly more favorable. Therefore, the transformation of the acylperoxo complex **2** may follow both pathways simultaneously to produce two unusual triplet Mn^V **2-cis-oxo** and one quintet **N-oxo** species. In the **2-trans** homolytic cleavage of the O−O bond produces Mn^{IV} **2-trans-oxo1** with bound RCO_2 radical and cannot compete with the two **cis** isomers.

4. The above-given third conclusion has been based on the results obtained at the hybrid B3LYP level, which overestimates the energies of the low spin states. Therefore, one may expect that at the pure density functional levels the entire reaction may take place in the triplet manifold with much lower barrier than the one predicted here for mixed spin state pathway.

5. For the most thermodynamically stable **N-oxo** product our calculations show that the energetic barrier (14.9 kcal/mol barrier) for its formation from the **2-cis(O,N)** acylperoxo complex (**2-cis(O,N)-TS1**) is by 4.3, 4.8, and 8.9 kcal/mol lower than those from the (Salen)Mn^VO,[71] **2-cis(O,N)-oxo** (**2-cis(O,N)-TS3**) and **2-trans** (**2-trans-TS1**) species, respectively. Therefore,

formation of **N-oxo** species from **2-cis(O,N)** acylperoxo complex is easier than from any **oxo**-species, as well as **2-trans** acylperoxo complex.

6. Cationic acylperoxo complex **3** does not undergo O−O bond cleavage, either in its high or low spin state.

Supporting Information Available: Tables 1S includes the Cartesian (x,y,z) coordinates of all optimized structures and their total energies. Tables 2S and 3S include the spin densities and Mulliken atomic charges of all calculated species, respectively. Table 4S composes relative energies and $<S^2>$ values required for Yamaguchi correction for all spin-broken species. In the Table 5S, the deformational energies of the complex fragments (salen and RCO_3) for selected states of all isomers of the complexes **2** and **3** are provided. In the Figures 1S, we depict the optimized structures and important geometries of the **2-cis-(O,N)-TS3**. This material is available free of charge via the Internet at http://pubs.acs.org.

JA0343656